ARTICLE

Magnetism and Sound Velocities of Iron Carbide (Fe_3C) under Pressure

Zhao-yi Zeng[a,b*], Cui-e Hu[a,b], Xun Liu[c], Ling-cang Cai[b]

a. College of Physics and Electronic Engineering, Chongqing Normal University, Chongqing 400047, China

b. National Key Laboratory for Shock Wave and Detonation Physics Research, Institute of Fluid Physics, Chinese Academy of Engineering Physics, Mianyang 621900, China

c. Institute of Pulsed Power Science, Kumamoto University, Kurokami, Kumamoto 860-8555, Japan

(Dated: Received on January 2, 2014; Accepted on April 11, 2014)

The elastic property and sound velocity of Fe_3C under high pressure are investigated by using the spin-polarized generalized gradient approximation within density-functional theory. It is found that the magnetic phase transition from the ground ferromagnetic (FM) state to the nonmagnetic (NM) state occurs at ~73 GPa. Based on the predicted Hugoniot of Fe_3C, we calculate the sound velocities of FM-Fe_3C and NM-Fe_3C from elastic constants. Compared with pure iron, NM-Fe_3C provides a better match of compressional and shear sound velocities with the seismic data of the inner core, supporting carbon as one of the light elements in the inner core.

Key words: Alloy, Sound velocity, Density functional theory

I. INTRODUCTION

The inner core is isolated from the rest of the Earth, which is the most remote and enigmatic part of our planet [1]. From seismic velocities, we know that the Earth's inner core is seismically anisotropic: compressional sound waves travel 3%−4% faster along the spin axis than in the equatorial plane [2]. The cause of the anisotropy has been generally attributed to preferential alignment of iron crystals. The density of the inner core is smaller than pure iron under corresponding pressure and temperature conditions. It is believed that the inner core is composed primarily of pure Fe or Fe-Ni alloy and other light elements, such as O, C, S, and H. Wood suggested that there might be a significant amount of C in the Earth's core [3]. Cementite (Fe_3C) is a proposed component. Aside from the practical importance in geology, the morphology of Fe_3C directly controls the mechanical properties of steels.

In the past few years, the scientific investigations on Fe_3C have been made extensively, including the structural properties [4, 5], elastic properties [6−8], magnetism [9−11], melting curves [12], sound velocities [9, 13−15], and so on. From the theoretical point of view, the previous investigations focused on the elastic constants under high pressure and zero temperature. Meanwhile, there were no available experimental measurements of the single-crystal elastic constants. In this work, we present the *ab initio* results for lattice parameters, magnetism and Hugoniot, and then obtain the elastic constants and sound velocities along Hugoniot. As the present results can be compared with the seismic data, it can help us understand the nature of the Earth's inner core.

*Author to whom correspondence should be addressed. E-mail: zhaoyizeng@126.com

II. COMPUTATIONAL METHOD

The structure calculations were carried out using the Vienna *ab initio* simulation package (VASP) [16], employing the density-functional theory (DFT) within the highly accurate frozen core all-electron projector-augmented wave (PAW) method [17]. Considering the magnetism of the Fe atom, we performed the spin-polarized *ab initio* calculations to investigate the structures, magnetism and phase transition of pure Fe under pressure successfully in previous work [18]. We also think spin-polarized method is also helpful for understanding Fe_3C. The exchange and correlation potentials were treated within the generalized gradient approximation (GGA) of Perdew-Burke-Ernzerhof (PBE) [19]. A plane-wave energy cutoff of 500 eV was used. The calculations were performed requiring a self-consistency convergence on the total energy of 10^{-6} eV per simulation cell. Brillouin zone integration was performed using k point sampling with 9×9×9 Monkhorst-Pack grid on the Fe_3C primitive cell. To obtain the equilibrium structures of unit cells at applied pressures, internal atomic positions were optimized until the residual forces became less than 10^{-3} eV/Å. To investigate the properties of Fe_3C at high temperature, we applied the quasi-harmonic Debye model [20, 21]. By this method, we have obtained the thermodynamics of Ti [22], Zr_2Al

DOI:10.1063/1674-0068/27/03/297-301

TABLE I The equilibrium lattice parameters a, b, c, volume V_0, zero pressure bulk modulus B_0, and pressure derivative B_0' at 0 GPa and 0 K.

		a/Å	b/Å	c/Å	V_0/Å^3	B_0/GPa	B_0'/GPa
This work	FM	5.021	6.768	4.432	150.489	195.570	5.804
	NM	4.925	6.648	4.382	143.483	289.269	5.022
Expt. [13]	FM	5.0816	6.7537	4.5139	154.90		
Expt. [30]	FM	5.091	6.743	4.526	155.4		
Calc. [7]	NM	4.921	6.644	4.378	143.26	297.0	4.9
Calc. [6]	FM	5.04	6.720	4.480	151.7		
Calc. [10]	FM	5.008	6.725	4.465	150.4		
Calc. [8]	FM	5.036	6.724	4.48	151.7		

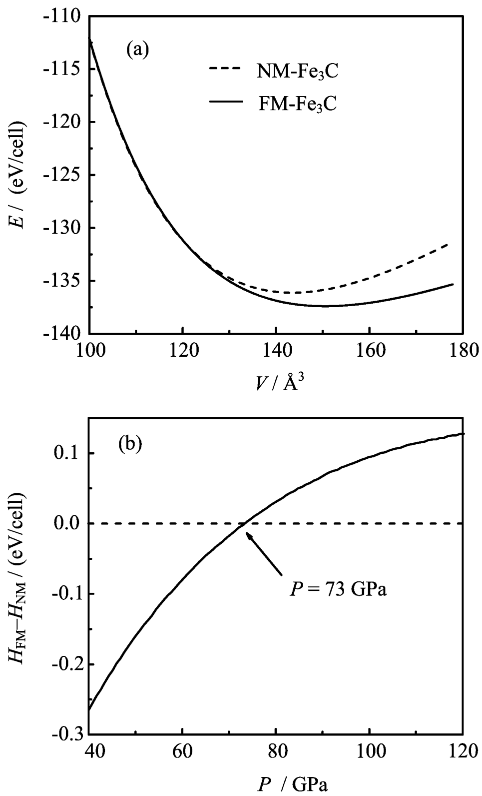

FIG. 1 (a) Static E-V data for FM-Fe_3C and NM-Fe_3C, (b) enthalpy difference between FM-Fe_3C and NM-Fe_3C.

[23], BC_2N [24], and NiTi alloy [25] under high pressure and high temperature successfully.

III. RESULTS AND DISCUSSION

At ambient conditions, Fe_3C has an orthorhombic structure. Synchrotron-based X-ray diffraction studies have shown that the crystal structure of Fe_3C remains stable up to 356 GPa and 5520 K [26]. So in the present work, the crystal structures of both ferromagnetic (FM) and nonmagnetic (NM) Fe_3C are treated as orthorhombic structure. We calculated the energy-volume (E-V) data of Fe_3C, which are shown in Fig.1. And then, these E-V data can be fitted to the Birch-Murnaghan equation of state (EOS) to obtain the static EOS [27, 28], such as bulk modulus B_0 and its pressure derivation B_0', pressure-volume-enthalpy (P-V-H) relations. From Fig.1, it can be seen that the ground state of Fe_3C is magnetism, and the E-V curves of both FM-Fe_3C and NM-Fe_3C are nearly the same below 129.5 Å^3. By computing the enthalpy difference $H_{\rm FM}-H_{\rm NM}$ at different pressures, we can find the critical pressure, where the $H_{\rm FM}-H_{\rm NM}$=0. It means that Fe_3C undergoes a magnetic transition under compression. By X-ray emission experiments, Lin *et al.* showed that the transition pressure located at around 25 GPa and 300 K, and the elastic properties also changed here [11]. But by X-ray diffraction and inelastic X-ray scattering experiments, the magnetic transition pressure was reported to be 68 GPa [9] and 55 GPa [4], respectively. Theoretically, Sata *et al.* found a smaller compressibility of Fe_3C above 50 GPa at room temperature [5], indicating the magnetic transition. Earlier first-principles calculations predicted magnetic collapse at 60 GPa [29]. In the present calculation, the magnetic transition pressure is ~73 GPa, close to our previous result (72.9 GPa) for fcc Fe [18]. Here, the transition can also be attributed to the high-spin to the low-spin transition of Fe atom.

The calculated equilibrium lattice parameters a, b, c, bulk modulus B_0 and its pressure derivation B_0' are listed in Table I, together with the experimental data [13, 30] and other theoretical results [6−8, 10], which are in good agreement. The pressure dependencies of the lattice parameters a, b, c for FM- and NM-Fe_3C are illustrated in Fig.2. By synchrotron X-ray diffraction experiments, Sata *et al.* found that as the magnetic transition, the measured EOS data above 50 GPa show a smaller compressibility than that below 25 GPa [5]. Whereas, Ono *et al.* found that the a- and c-axes decreased continuously as the pressure increased [4]. In contrast, the b-axis showed a discontinuity in its reduction at 55 GPa. About 1.7% reduction in volume was observed. It is obvious that the results for FM state agree with the experimental data at low

DOI:10.1063/1674-0068/27/03/297-301

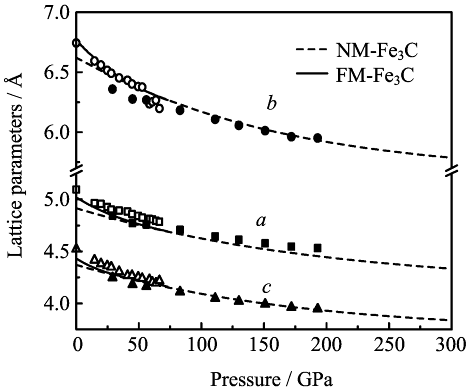

FIG. 2 Lattice parameters a, b, c of Fe_3C. The solid and open symbols are X-ray diffraction data taken from Sata *et al.* [5] and Ono *et al.* [4], respectively.

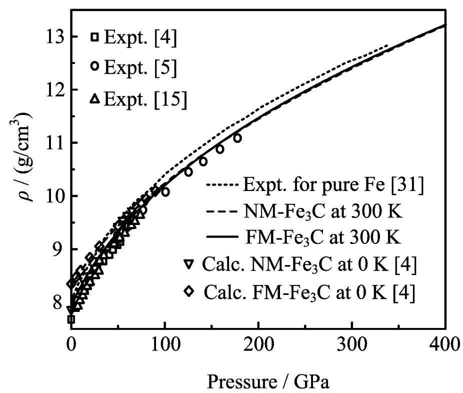

FIG. 3 300 K EOS of FM- and NM-Fe_3C, together with the experimental data [4, 5, 15] and theoretical results [4].

pressure, and the agreement between present NM state and experiments at higher pressure is satisfactory [4, 5]. In the present work, the volume from FM phase to NM phase is continuous around the transition pressure, which agrees with the conclusion from *ab initio* calculations by Ono *et al.* [4]. It is expected that the magnetic transition is a second-order transition [29].

The isotherms of FM- and NM-Fe_3C at 300 K are shown in Fig.3. Our results are in reasonable accordance with experiments [4, 5, 15] and pervious calculations [4]. At lower pressure (0−73 GPa), our results for FM-Fe_3C agree well with the experimental data [4, 5, 15]. While at higher pressure (>73 GPa), the 300 K isotherms of FM- and NM-Fe_3C are nearly coincident, which indicates the FM→NM transition. The present density data are smaller than pure Fe at all range of pressures [31]. In order to estimate whether the Fe_3C could be treated as a candidate under Earth's core condition, it is necessary to obtain density data under pressure-temperature conditions close to those of the inner core.

In shock wave (SW) experiment, conservation of mass, momentum and energy requires that the pressure P_H, the molar internal energy U_H, and the molar volume V_H in the compression wave are related by the Rankine-Hugoniot formula

$$U_\mathrm{H} - U_0 = \frac{1}{2}\left(P_\mathrm{H} + P_0\right)\left(V_0 - V_\mathrm{H}\right) \tag{1}$$

where U_0 and V_0 are the molar internal energy and volume in the initial state (zero-pressure P_0) before the arrival of the shock wave. The quantities measured directly are the shock-wave and material velocities, which allow the values of P_H and V_H to be deduced. Hugoniot curve is one of the fundamental properties of material, which can reflect the response of material to both pressure and temperature. According to Eq.(1), we obtained the P_H-V_H relation along the Hugoniot, and here we translated V_H to density (ρ). As shown in Fig.4, the present Hugoniot of Fe_3C generally agree with the Hugoniot of cast iron [32]. At low pressure, the densities of NM-Fe_3C along Hugoniot are larger than that of FM-Fe_3C. Under higher pressure, the differences become smaller. Under the Earth's core pressure, compared with the density of Fe along Hugoniot [33], the present data of NM-Fe_3C are closer to preliminary earth reference model (PREM) data [34]. Figure 4 also shows the obtained Hugoniot P-T. Unfortunately, there are no available Hugoniot P-T data for Fe_3C. So, we list the theoretical data for pure iron for comparison. The P-T

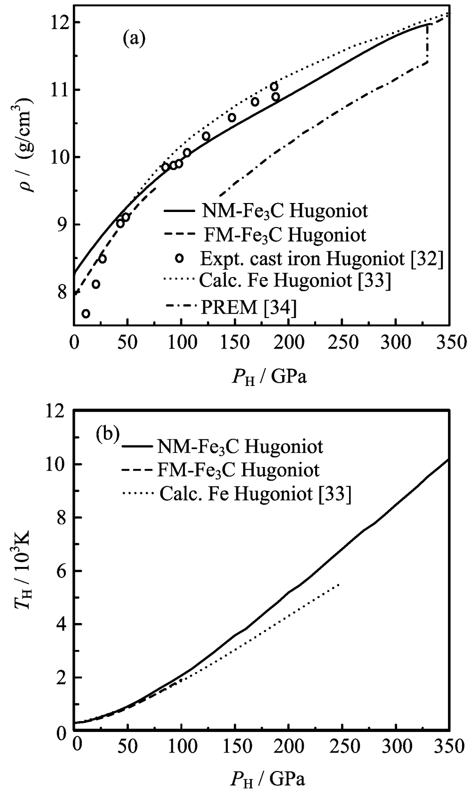

FIG. 4 (a) P_H-ρ and (b) P_H-T_H of FM-Fe_3C and NM-Fe_3C along Hugoniot, together with the experimental data for cast iron [32], theoretical results for Fe [33] and PREM data [34].

DOI:10.1063/1674-0068/27/03/297-301

TABLE II The elastic constants C_{ij} (in GPa) of Fe_3C at static equilibrium volume.

		C_{11}	C_{22}	C_{33}	C_{44}	C_{55}	C_{66}	C_{12}	C_{13}	C_{23}
This work	NM	514.1	480.8	520.3	1.4	162.8	168.7	242.4	242.9	198.9
	FM	393.4	357.2	323.1	41.8	143.1	152.7	148.9	144.2	156.0
Calc. [7]	NM	479.5	442.8	479.5	−6.0	149.4	152.6	236.7	236	187.7
Calc. [6]	FM	395	347	325	18	134	135	158	169	163
Calc. [8]	FM	385	341	353	13	131	131	157	162	167

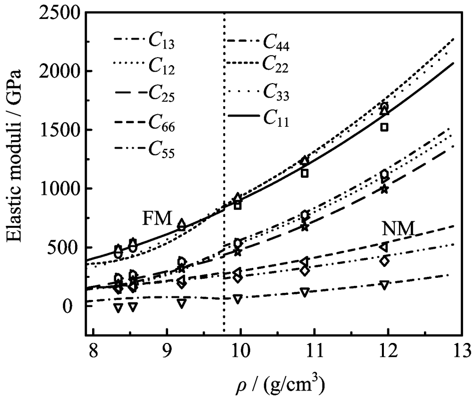

FIG. 5 Elastic constants versus density, the open symbols are taken from *ab initio* calculations by Mookherjee [7].

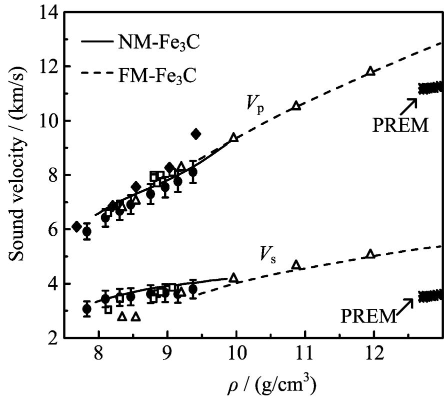

FIG. 6 Sound velocities of Fe_3C under density, the open triangles are from *ab initio* calculation [7], the solid circles [13], open squares [14], solid diamonds [9] are experimental data, and the crosses are from PREM [34].

curve of FM-Fe_3C agrees with the data for Fe predicted by Alfè *et al.* [33]. The Hugoniot temperatures of NM-Fe_3C are larger than that of FM-Fe_3C. Though there are no experimental data for comparison, we conclude the present results may overestimate the temperature under high pressure. The main factor leading to an overestimation of the temperature is our neglecting of the anharmonicity in present calculations.

Apart from the density of the inner core, the solid phase must have appropriate sound velocities. So we also calculated the sound velocities at different volumes. To calculate the compressional sound velocity V_p and shear sound velocity V_s, we use the formulas as follows:

$$V_\mathrm{p} = \sqrt{\frac{B + 4G/3}{\rho}} \qquad (2)$$

$$V_\mathrm{s} = \sqrt{\frac{G}{\rho}} \qquad (3)$$

where ρ is the density, B and G are bulk and shear modulus which can be calculated from the elastic constants according to Voigt-Reuss-Hill approximations [35]. At static equilibrium volume, the present elastic constants are shown in Table II. In comparison with the results for FM-Fe_3C, the NM elastic constants are stiffer. We evaluated the full elastic constants of FM- and NM-Fe_3C at different density (volume). The elastic constants of both FM- and NM-Fe_3C increase monotonically with density (Fig.5), except for the shear elastic constant C_{44} for FM phase. In present calculations, the FM C_{44} increase firstly and then decease with the increased density (or pressure), and the variation generally agree with the results by Mookherjee *et al.* [7]. The largest FM C_{44} is 76.16 GPa at 8.93 g/cm^3. This might be related to the resistance to shearing by the aligned spins in FM phase [7].

The present results on the sound velocities of compressed Fe_3C at different densities (Fig.6) agree with previous experiments [9, 13, 14]. At zero pressure (the density is 7.96 g/cm^3), the V_p and V_s of FM-Fe_3C are 6.63 and 3.31 km/s, respectively. The maximum V_s (3.99 km/s) for FM-Fe_3C located at 9.46 g/cm^3, corresponding to a Hugoniot pressure of 71.5 GPa. If the density increases continuously, the V_s for FM-Fe_3C will decrease. The V_s of NM-Fe_3C are larger than that of FM-Fe_3C at low pressure. For the sound velocities V_p, the data of both FM- and NM-Fe_3C in present calculations increase with the increased density. A test for Fe_3C as a component of the inner core is to compare its sound velocities with the PREM values [34]. In the Earth's inner core condition, the V_p and V_s data of Fe_3C is about 12.1 and 5.1 km/s, which are larger than that of PREM values. Extrapolating to the density of the inner core, the V_p and V_s of Fe_3C are ∼0.8 and ∼1.5 km/s which are lower than the data of pure Fe measured by

DOI:10.1063/1674-0068/27/03/297-301

Mao *et al.* [36]. The remaining difference of ~1.5 km/s (V_p) and 1.6 km/s (V_s) may be accounted for the presence of other light elements (such as S and O) and heavy element alloy (such as 5% to 10% Ni). In order to understand the seismic data, further systematic studies are needed to improve our knowledge. For instance, the disordered iron-carbon alloys and iron-nickel-light element alloys should be considered, as Fe_3C in this work is an ordered and alloyed cementite.

IV. CONCLUSION

In summary, we extensively studied the elastic properties and sound velocity of Fe_3C under high pressure and high temperature by using the spin-polarized generalized gradient approximation within density functional theory. It is found that the magnetic phase transition from the ground FM state to the NM state occurs at ~73 GPa. Within the quasi-harmonic Debye approximation, we predicted the Hugoniot of Fe_3C. And then we obtained the sound velocities of FM- and NM-Fe_3C from the calculated elastic constants. Compared with pure iron, Fe_3C provides a better match of compressional and shear sound velocities to the seismically data of the inner core, supporting carbon as one of light elements in the inner core. These investigations will be very useful for studying the properties of the Earth's inner core.

V. ACKNOWLEDGMENTS

This work was supported by the National Natural Science Foundation of China (No.11247316, No.11247317, No.11347019, No.11304408, and No.U1230201), the Science and Technology Research Project of Chongqing Education Committee (No.KJ120613 and No.KJ130607), and the Natural Science Foundation of Chongqing City (No.cstc2012jjA50019 and No.cstc2013jcyjA0733).

[1] D. L. Anderson, Proc. Natl. Acad. Sci. USA **99**, 13966 (2002).
[2] K. C. Creager, Nature **356**, 309 (1992).
[3] B. J. Wood, Earth Planet. Sci. Lett. **117**, 593 (1993).
[4] S. Ono and K. Mibe, Phys. Earth Planet. In. **180**, 1 (2010).
[5] N. Sata, K. Hirose, G. Y. Shen, Y. Nakajima, Y. Ohishi, and N. Hirao, J. Geophys. Res. **115**, B0920 (2010).
[6] C. Jiang, S. G. Srinivasan, A. Caro, and S. A. Maloy, J. Appl. Phys. **103**, 043502 (2008).
[7] M. Mookherjee, Am. Mineral. **96**, 1530 (2011).
[8] M. Nikolussi, S. L. Shang, T. Gressmann, A. Leineweber, E. J. Mittemeijer, Y. Wang, and Z. K. Liu, Scr. Mater. **59**, 814 (2008).
[9] G. Fiquet, J. Badro, E. Gregoryanz, Y. Fei, and F. Occelli, Phys. Earth Planet In. **172**, 125 (2009).
[10] Z. Q. Lv, F. C. Zhang, S. H. Sun, Z. H. Wang, P. Jiang, W. H. Zhang, and W. T. Fu, Comp. Mater. Sci. **44**, 690 (2008).
[11] J. F. Lin, V. V. Struzhkin, H. K. Mao, and R. J. Hemley, Phys. Rev. B **70**, 212405 (2004).
[12] O. T. Lord, M. J. Walter, R. Dasgupt, D. Walker, and S. M. Clark, Earth Planet Sci. Lett. **284**, 157 (2009).
[13] L. Gao, B. Chen, M. Lerche, E. E. Alp, W. Sturhahn, J. Zhao, H. Yavas, and J. Li, J. Synchrotron Rad. **15**, 714 (2009).
[14] L. Gao, B. Chen, J. Zhao, E. E. Alp, W. Sturhahn, and J. Li, Earth Planet Sci. Lett. **309**, 213 (2011).
[15] L. L. Gao, B. Chen, J. Y. Wang, E. E. Alp, J. Y. Zhao, M. Lerche, W. Sturhahn, H. P. Scott, F. Huang, Y. Ding, S. V. Sinogeikin, C. C. Lundstrom, J. D. Bass, and J. Li, Geophys. Res. Lett. **35**, L17306 (2008).
[16] G. Kresse and J. Furthmüller, Phys. Rev. B **54**, 11169 (1996).
[17] P. E. Blöchl, Phys. Rev. B **50**, 17953 (1994).
[18] Z. Y. Zeng, C. E. Hu, X. R. Chen, L. C. Cai, and F. Q. Jing, J. Phys.: Condens. Matter **20**, 425217 (2008).
[19] J. P. Perdew, K. Burke, and M. Ernzerhof, Phys. Rev. Lett. **77**, 3865 (1996).
[20] M. A. Blanco, A. M. Pendás, E. Francisco, J. M. Recio, and R. Franco, J. Mol. Struct.: THEOCHEM **368**, 245 (1996).
[21] M. Flórez, J. M. Recio, E. Francisco, M. A. Blanco, and A. M. Pendás, Phys. Rev. B **66**, 144112 (2002).
[22] C. E. Hu, Z. Y. Zeng, L. Zhang, X. R. Chen, L. C. Cai, and D. Alfè, J. Appl. Phys. **107**, 093509 (2010).
[23] X. L. Yuana, D. Q. Wei, Y. Cheng, Q. M. Zhang, and Z. Z. Gong, J. At. Mol. Sci. **3**, 160 (2012).
[24] J. Chang, Y. Cheng, and M. Fu, J. At. Mol. Sci. **1**, 243 (2010).
[25] Z. Y. Zeng, C. E. Hu, L. C. Cai, X. R. Chen, and F. Q. Jing, Solid State Commun. **149**, 2164 (2009).
[26] S. Tateno, K. Hirose, Y. Ohishi, and Y. Tatsumi, Science **330**, 359 (2010).
[27] F. Birch, Phys. Rev. **71**, 809 (1947).
[28] F. Birch, J. Geophys. Res. **83**, 1257 (1978).
[29] L. Vočadlo, J. Brodholt, D. P. Dobson, K. S. Knight, W. G. Marshall, G. D. Price, and I. G. Wood, Earth Planet Sci. Lett. **203**, 567 (2002).
[30] J. Li, H. K. Mao, Y. Fei, E. Gregoryanz, M. Eremets, and C. S. Zha, Phys. Chem. Miner. **29**, 166 (2002).
[31] H. K. Mao, Y. Wu, L. C. Chen, J. F. Shu, and A. P. Jephcoat, J. Geophys. Res. **95**, 21737 (1990).
[32] S. P. Marsh, *Los Alamos Shock Hugoniot Data*, Berkeley: University of California Press, (1980).
[33] D. Alfè, G. D. Price, and M. J. Gillan, Phys. Rev. B **65**, 165118 (2002).
[34] A. Dziewonski and D. L. Anderson, Phys. Earth Planet. Inter. **25**, 297 (1981).
[35] R. Hill, Proc. Phys. Soc. London **65**, 350 (1952).
[36] H. K. Mao, J. Xu, V. V. Struzhkin, J. Shu, R. J. Hemley, W. Sturhahn, M. Y. Hu, E. E. Alp, L. Vočadlo, D. Alfè, G. D. Price, M. J. Gillan, M. Schwoerer-Böhning, D. Häusermann, P. Eng, G. Shen, H. Giefers, R. Lübbers, and G. Wortmann, Science **292**, 914 (2001).

DOI:10.1063/1674-0068/27/03/297-301